IEEE Access
Multidisciplinary | Rapid Review | Open Access Journal

Received February 5, 2018, accepted March 9, 2018, date of publication March 23, 2018, date of current version April 23, 2018.

Digital Object Identifier 10.1109/ACCESS.2018.2818743

Design of Compact Bandpass Filters Using Novel Dual-Mode Dielectric Patch Resonator

JIAN-XIN CHEN[1,2], (Senior Member, IEEE), YUN-LI LI[1,2], WEN-WEN YANG[1,2], AND ZHI-HUA BAO[1,2]

[1]School of Electronics and Information, Nantong University, Nantong 226019, China
[2]Nantong Research Institute for Advanced Communication Technologies, Nantong 226019, China

Corresponding author: Jian-Xin Chen (jjxchen@hotmail.com)

This work was supported in part by the National Natural Science Foundation of China under Grant 61501263 and Grant 61371111, in part by the Natural Science Foundation of Jiangsu Province, China, under Grant BK20161281, and in part by the Nantong University-Nantong Joint Research Center for Intelligent Information Technology.

ABSTRACT This paper introduces a new dual-mode dielectric patch resonator (DPR), which consists of a thin square dielectric patch with high permittivity and a low-permittivity substrate with bottom ground plane. A pair of TM_{11} degenerate modes can act as the dominate mode by fusing the dielectric patch and the substrate with the ground plane, whose resonant frequency is derived by using the combination of mixed magnetic wall method and mirror theory. It can be found that the constructed dual-mode DPR owns both merits of the planar transmission line and the dielectric resonator at the same time, i.e., low-profile configuration and high unloaded quality factor (Q_u). Based on the proposed dual-mode DPR, a single-ended bandpass filter (BPF) and a differential BPF is designed respectively. Good agreement can be observed between their respective simulated and measured results. Both of them showcase several advantages such as low passband loss, low profile, and compact size.

INDEX TERMS Dielectric patch resonator (DPR), bandpass filter (BPF), dual-mode, low profile, unloaded quality factor Q_u.

I. INTRODUCTION

The dielectric resonators (DRs) with high permittivity have been widely applied in modern wireless communication systems, such as cellular base station and satellite payloads, owing to their high unloaded-Q factor, high power capacity, and superior temperature stability, etc. [1]–[5]. In the past several decades, various high-performance microwave components and circuits based on the DRs, such as multiplexers [6], [7], oscillators [8], [9], antennas [10]–[14] and filters [15]–[25], have been developed. In the designs of DR filters, the most commonly employed DR structures are classified into two types: (1) Individual DR loaded in a metallic cavity, in which the support is necessary for the DR [19]–[23]. (2) DR with small height mounted on the planar substrate with low permittivity [24], [25]. In the former case, good performance of the filters in either single-ended or differential topology can be obtained easily, such as low insertion loss and sharp skirt selectivity because the high unloaded-Q factor (Q_u) of the DR is maintained. To reduce the filters' volume, various dual-/multi-mode DRs are extensively explored for replacing two or more cascaded single-mode DRs [17]–[20]. However, these filters still exhibit high profile and difficulty in integration with other planar circuits.

In the latter case, the DRs are put on the substrate using the low permittivity and low loss materials, which can effectively alleviate the problematic issues mentioned above. In the most designs [24], [25], the dominate TE mode is utilized and the substrate has rare effect on the DR because the E-field is confined in the DR. As a result, the substrate only acts as a support for the DR. Recently, the dielectric patch resonator (DPR) is developed to design low-profile antennas with enhanced bandwidth [26]–[28]. The single TM mode of the DPR is employed, but the rigorous analysis for the mode characteristics is not mentioned.

In this paper, a dual-mode DPR is constructed for the first time and theoretically investigated for designing compact bandpass filters (BPFs). A thin square dielectric patch is put on the low-permittivity substrate with bottom ground plane, and a pair of TM_{11} degenerate modes can replace the traditional TE_{11} mode to be the dominate mode by fusing

the dielectric patch and the substrate. And then the designed dual-mode DPR processes both merits of the planar transmission line and the DR simultaneously, i.e. low-profile configuration and high Q_u. Finally, the proposed dual-mode DPR is successfully applied to design single-ended and differential BPFs, and their simulated and measured results with good agreement are presented.

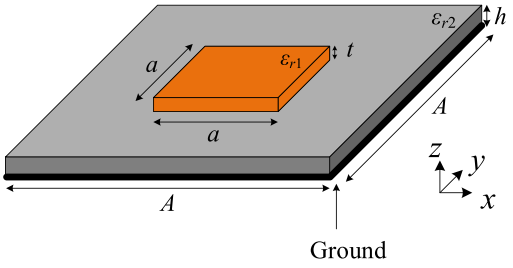

FIGURE 1. Schematic layout of the proposed square DPR.

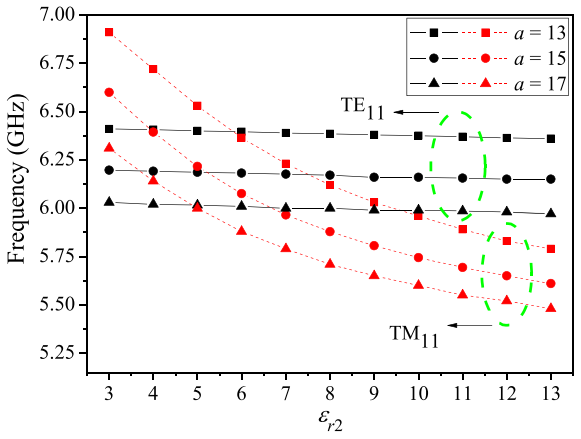

FIGURE 2. The resonant frequencies of TE_{11} and TM_{11} modes against ε_{r2} under different a, while ε_{r1} = 90, t = 1.0mm and h = 0.76mm are fixed.

II. THEORETICAL ANALYSIS OF THE PROPOSED DPR

Fig. 1 shows the configuration of the proposed DPR, which consists of a thin square dielectric patch with a high dielectric constant ε_{r1} (loss tangent tanδ_1) and a volume of $a \times a \times t$, and a substrate with a low dielectric constant ε_{r2} (loss tangent tanδ_2) and a volume of $A \times A \times h$. There is a metallic ground plane on the bottom layer of the substrate. For the DR with the rectangular/square shape, it is well known that there are multiple resonant modes, such as TE_{11}, TM_{11} and other high-order modes. Generally, the TE_{11} mode of the DR is the dominate one when the ratio of t/a is small, as described by many previous works [24], [25]. Meanwhile, since the E-field of the TE_{11} mode is mainly concentrated in the DR body, the substrate with the bottom ground plane underneath the DR has rare influence on it, as shown in Fig. 2. However, the TE_{11} mode is used as a single-mode operation, which goes against the miniaturization of the circuit. On the other hand, the TM_{11} mode usually acts as the lowest spurious mode of the DR, and its E-field mainly distributes along z direction while part of field distributes outside of the DR. Thus, the TM_{11} mode will be affected by the substrate with the bottom ground plane significantly. As ε_{r2} of the substrate increases, the resonant frequency of TM_{11} mode drops dramatically while that of TE_{11} mode keeps unchanged almost. Therefore, it is predictable that the TM_{11} mode can function as the dominate mode by choosing the proper parameters of the proposed DPR. The detailed analysis for the DPR with TM_{11} dominate mode is given below.

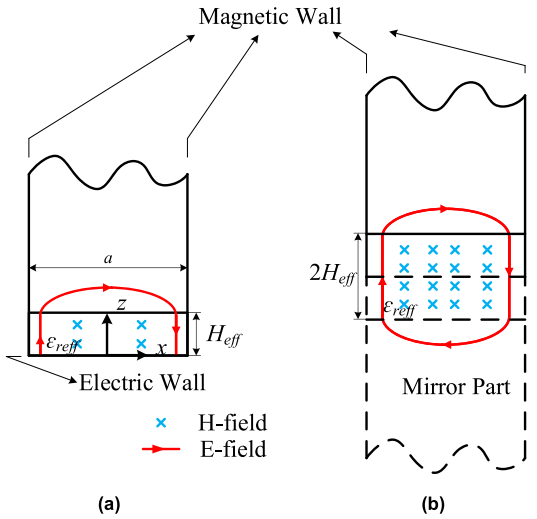

FIGURE 3. The analysis models for TM_{11} mode, (a) established DR model of the proposed DPR, (b) equivalent DR model mirrored from the model in Fig. 3(a).

Fig. 3(a) shows the analysis model of the proposed square DPR, where a new DR with an effective dielectric constant ε_{reff} and a thickness of H_{eff} is established for the investigation. When $\varepsilon_{r1} >> \varepsilon_{r2}$ and $t > h$ (small value), it is assumed that

$$\varepsilon_{reff} = (t \cdot \varepsilon_{r1} + h \cdot \varepsilon_{r2})/(t + h) \quad (1)$$

$$H_{eff} = t + h \quad (2)$$

Accordingly, the ε_{reff} of the new DR is still high enough so that the four side planes of the DR along z direction can also be treated as magnetic wall for analysis according to the traditional mixed magnetic wall method. The bottom ground plane of the new DR can be considered as a electrical wall. According to the E-field distribution of the TM_{11} mode of the DR, the model in Fig. 3(a) can be symmetrically mirrored with respect to the electrical wall (ground plane), resulting in an equivalent DR in Fig. 3(b). As a result, the complicated DPR in Fig.1 is converted to a traditional DR for solving the

TM_{11} mode, which can be expressed as

$$\begin{cases} E_x = \dfrac{1}{k^2+\gamma_z^2}\dfrac{\partial^2 E_z}{\partial x \partial z}, E_y = \dfrac{1}{k^2+\gamma_z^2}\dfrac{\partial^2 E_z}{\partial y \partial z} \\ H_x = \dfrac{j\omega\varepsilon}{k^2+\gamma_z^2}\dfrac{\partial E_z}{\partial y}, H_y = -\dfrac{j\omega\varepsilon}{-k^2+\gamma_z^2}\dfrac{\partial E_z}{\partial x} \end{cases}$$

$$E_z = \begin{cases} A_1 \cos k_x x \cdot \cos k_y y \cdot \cos(k_z z + \varphi) \\ \quad -H_{eff} \le z \le H_{eff} \\ A_2 \cos k_x x \cdot \cos k_y y \cdot e^{-\alpha_z (z - H_{eff})} \\ \quad z \ge H_{eff} \\ A_3 \cos k_x x \cdot \cos k_y y \cdot e^{-\alpha_z (z + H_{eff})} \\ \quad z \le -H_{eff} \end{cases}$$

$$k_x^2 + k_y^2 + k_z^2 = \varepsilon_{reff} k_0^2 \quad -H_{eff} \le z \le H_{eff}$$

$$k_x^2 + k_y^2 - \alpha_z^2 = k_0^2 \quad z \ge -H_{eff} \,\&\, z \le H_{eff}$$

$$k_x = \pi/a, k_y = \pi/a, k_z = (s+\delta)\pi/2H_{eff} \quad (3)$$

where ε is the permittivity in vacuum, k is the wave number at operation frequency and γ_z is the propagation constant along z direction. And the resonant frequency f_0 of the TM_{11} mode can be calculated from

$$k_x = k_y = \pi/a \quad (4)$$

$$k_z H_{eff} = \tan^{-1}\left(\frac{\varepsilon_{reff}\alpha_z}{k_z}\right) \quad (5)$$

$$k_x^2 + k_y^2 - \alpha_z^2 = k_0^2 \quad (6)$$

$$k_z^2 + \alpha_z^2 = (\varepsilon_{reff} - 1)k_0^2 \quad (7)$$

$$f_0 = \frac{c}{2\pi\sqrt{\varepsilon_{reff}}}\sqrt{k_x^2 + k_y^2 + k_z^2} \quad (8)$$

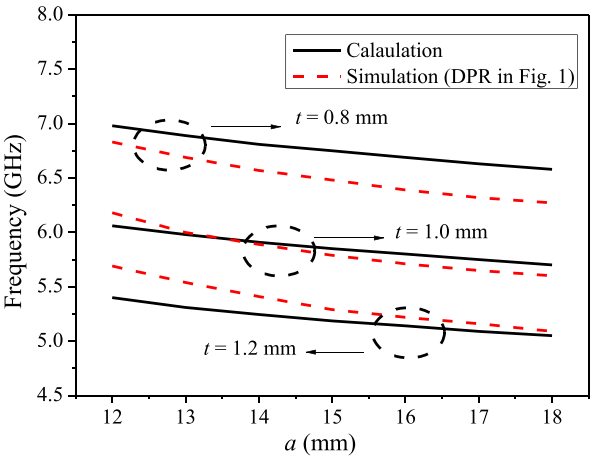

FIGURE 4. The calculated and simulated TM_{11} mode resonant frequencies under different a and t, while $\varepsilon_{r1} = 90$, $\varepsilon_{r2} = 9$ and h = 0.76mm are fixed.

Fig. 4 shows the calculated results of the model in Fig. 3(b) and the simulated results of the DPR in Fig. 1 under different a and t. It can be found that the simulated and the calculated results show good agreement, and the error between them is less than 5%, which effectively validates that the above assumption and mirror are reasonable (it should be noted that the parameters h and t have the same trend of the effect on

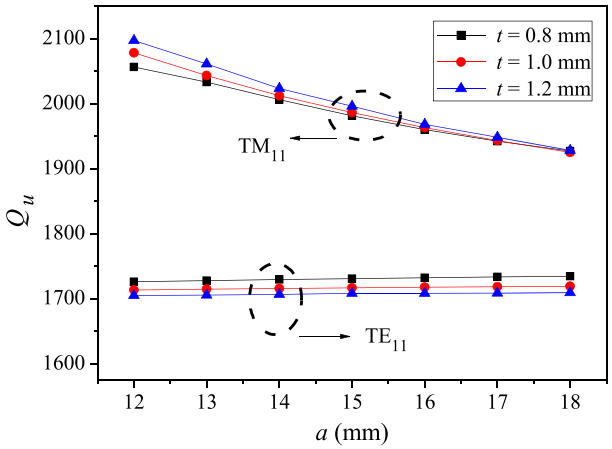

FIGURE 5. The extracted Q_u s of TM_{11} mode and TE_{11} mode of the proposed DPR under different a and t. while $\varepsilon_{r1} = 90$, $\varepsilon_{r2} = 9$, $\tan\delta_1$ = 6e-4, $\tan\delta_2$ = 1.5e-4 and h = 0.76mm are fixed.

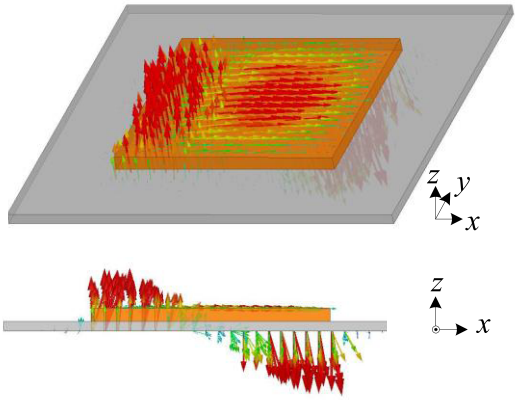

FIGURE 6. The E-field distribution of the TM_{11} mode.

f_0 according to (1) and (2), and the parameter A has no effect on it.). Fig. 5 shows the simulated Q_us of the TM_{11} mode and TE_{11} mode of the proposed DPR under different a and t. The Q_u of the TM_{11} mode keeps almost the same as t varies, enabling the easy construction of the low-profile DPR. It can also be found that the Q_u of about 2000 at 5.8GHz for the TM_{11} mode is about 5 $\sim$ 10 times that of the microstrip counterparts. Thus, the constructed DPR owns both merits of the planar transmission line and the DR at the same time, i.e. low-profile configuration and high Q_u. Fig. 6 shows the simulated E-field of the TM_{11} mode, which is similar with that of the microstrip half-wavelength patch resonator. Thus, the design method of the traditional microstrip filter can be applied to guide the proposed designs. Meanwhile, more design freedom of the proposed DPR can be obtained, e.g. the thickness and dielectric constant of the dielectric patch.

III. DESIGN OF SINGLE-ENDED FILTER

A. FILTER DESIGN

Fig. 7 shows the layout of the single-ended BPF constructed by the proposed dual-mode DPR in a metallic cavity and a pair of feeding probes, where ε_{r1} = 90 ($\tan\delta_1$ = 6e-4),

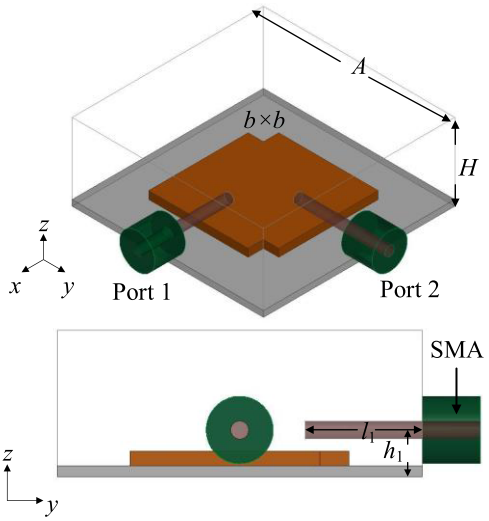

FIGURE 7. The layout of the single-ended BPF using the proposed dual-mode DPR.

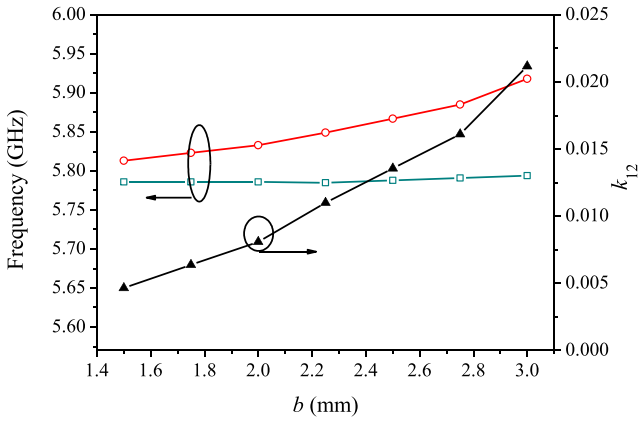

FIGURE 8. The frequency splitting of the two TM_{11} modes and k_{12} against the cut size b.

$\varepsilon_{r2} = 9$ ($\tan\delta_2 = 1.5\text{e-}4$), and $h = 0.76$mm are fixed. Like the dual-mode microstrip patch filter, the proposed DPR possesses two orthogonal TM_{11} modes in x and y directions, which are degenerate. Accordingly, a pair of cuts with the size $b \times b$ on the opposite corners are used for splitting the two degenerate TM_{11} modes, as shown in Fig. 8. As b increases, the frequency difference between the two modes is enlarged, meaning the coupling level between them is enhanced. Accordingly, the single-ended dual-mode BPF with a center frequency of $f_0 = 5.8$ GHz and a 0.1-dB ripple fractional bandwidth (FBW) of 0.8% is designed. According to the specifications, the lumped-element values of a low-pass prototype filter can be calculated as $g_1 = 0.89$, $g_2 = 0.64$ and $g_3 = 1.40$. Then, the required coupling coefficient k_{12} and the external quality factor Q_e can be obtained [29].

$$k_{12} = \frac{FBW}{\sqrt{g_1 g_2}} = 0.0107 \tag{9}$$

$$Q_e = \frac{g_0 g_1}{FBW} = 110.6 \tag{10}$$

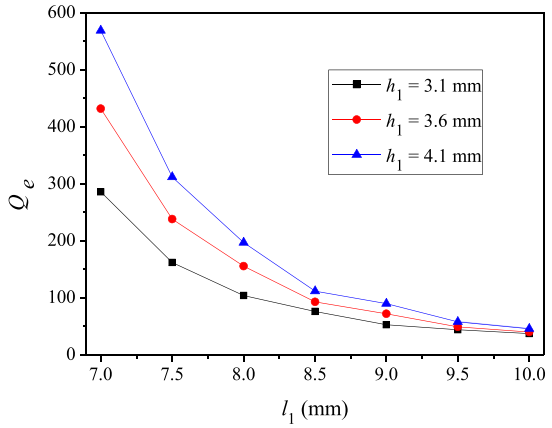

FIGURE 9. The relationship between Q_e and l_1 under different h_1.

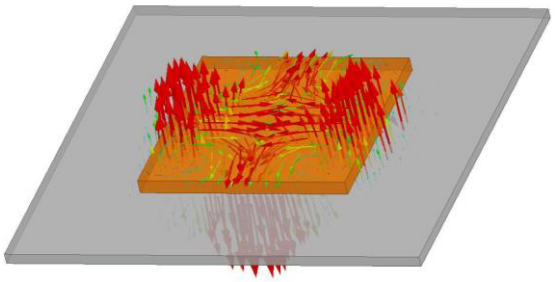

FIGURE 10. The E-field distribution of the TM_{22} mode.

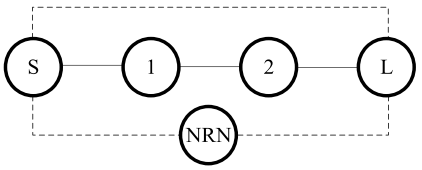

FIGURE 11. The coupling route of the proposed single-ended BPF.

The Q_e is mainly determined by the parameters of the feeding probe, i.e. l_1 and h_1, which can be tuned for meeting the requirement of the desired Q_e, as shown in Fig. 9. Once they are determined according to the desired Q_e, the cross coupling from source to load will be determined accordingly which should generate a pair of transmission zeros on the both sides of the passband. Unfortunately, the TM_{22} mode of the proposed DPR can also be well excited by the feeding probes according to its E-filed distribution shown in Fig. 10. It functions as a non-resonating node (NRN, i.e. resonating mode far away from the TM_{11} mode in spectrum, and it can be indicated as $M_{\mathrm{NRN}} = (f_0^2 - f_{\mathrm{NRN}}^2)/(\mathrm{FBW} \cdot f_0 \cdot f_{\mathrm{NRN}})$ in the coupling matrix, where f_{NRN} is the resonant frequency of the NRN) and then produces another cross coupling path for the filter. As a result, there is no transmission zero in the upper stopband. Fig. 11 shows the coupling route of the proposed BPF, where the solid line represents the main coupling while the dash line represents the cross coupling.

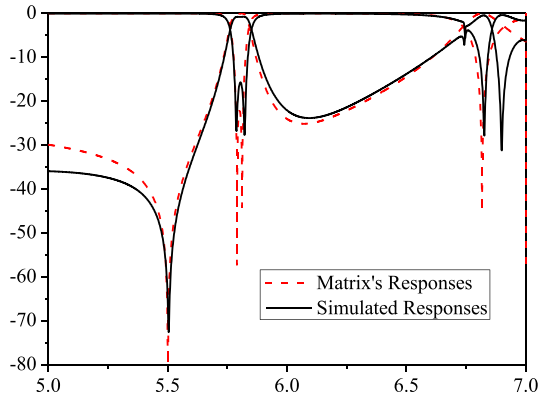

FIGURE 12. The frequency responses resulting from the coupling Matrix and HFSS simulation.

The coupling matrix M is adopted and shown below [30]:

$$M = \begin{bmatrix} & S & 1 & NRN & 2 & L \\ S & 0 & 0.81 & -0.96 & 0 & -0.02 \\ 1 & 0.81 & 0 & 0 & 0.707 & 0 \\ NRN & -0.96 & 0 & -39.9 & 0 & -0.96 \\ 2 & 0 & 0.707 & 0 & 0 & 0.81 \\ L & -0.02 & 0 & -0.96 & 0.81 & 0 \end{bmatrix} \tag{11}$$

Fig. 12 shows the frequency responses resulting from the matrix M in (11) and simulation of Ansoft HFSS, showing good accordance.

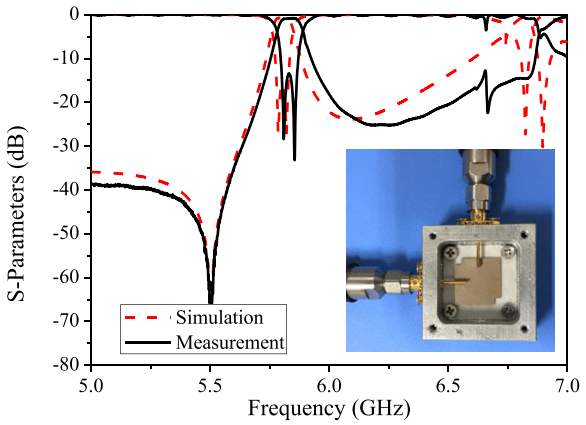

FIGURE 13. The simulated measured frequency responses of the proposed single-ended BPF (The inset is the photograph of fabricated BPF).

B. RESULT

According to the above discussion, the dimensions of the proposed single-ended BPF in Fig. 7 can be determined as: $A = 25$ mm, $H = 10$ mm, $a = 15$ mm, $b = 2.5$ mm, $t = 1$ mm, $h = 0.76$ mm, $h_1 = 3.6$ mm and $l_1 = 8.5$ mm. The experiment is carried out by using Agilent N5230A PNA-L network analyzer. Fig. 13 shows the simulated and measured results of the designed single-ended BPF (the inset photograph is the fabricated BPF), exhibiting good agreement. In experiment, the center frequency of the passband is about 5.83 GHz and the 3-dB FBW is around 1.8%. In the passband, the measured minimum insertion loss is 0.82 dB and the return loss is better than 13 dB.

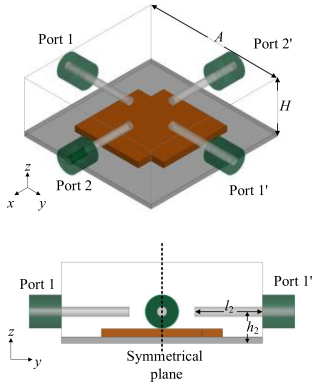

FIGURE 14. The schematic layout of the proposed differential BPF using the proposed DPR.

IV. DESIGN OF DIFFERENTIAL FILTER

A. FILTER DESIGN

Fig. 14 shows the configuration of the differential BPF, which consists of the proposed DPR loaded in a square metallic cavity and two pairs of differential ports, i.e. Port 1 and Port 1', and Port 2 and Port 2'. According to the E-field distribution, the TM_{11} mode can be differential excited for forming the differential passband. Meanwhile, the E-field distribution of TM_{22} mode (acting as the lowest spurious mode in the single-ended filter in Fig. 7) is even symmetric with respect to the symmetrical plane in Fig. 14. Thus, the TM_{22} mode acts as common-mode (CM) response, implying that the differential-mode (DM) upper stopband can be improved. When the proposed BPF is fed by one differential port pair, its perpendicularly symmetrical plane (along the other differential port pair) can be treated as a virtual ground. For example, the symmetrical plane in Fig. 14 is a virtual ground when the DM signal is fed through Port 1 and Port 1'. As a result, the isolation between the two differential port pairs is very high, as shown in Fig. 15. Therefore, the S-L coupling existing in the single-ended BPF in Fig. 7 (which can also be seen from Fig. 15) would disappear in the differential design. Accordingly, the coupling route of the proposed differential filter is very simple and shown in Fig. 16.

For demonstration, a differential dual-mode BPF with a center frequency of $f_0 = 5.8$ GHz and a 0.05-dB ripple FBW of 0.5% is designed. According to the specifications, the lumped-element values of a low-pass prototype filter can be obtained as $g_1 = 0.45$, $g_2 = 0.41$ and $g_3 = 1.10$. Then, the required coupling coefficient k_{12d} and the external quality factor Q_{ed} for the DM BPF can be obtained.

$$k_{12d} = \frac{FBW}{\sqrt{g_1 g_2}} = 0.0115 \tag{12}$$

$$Q_{ed} = \frac{g_0 g_1}{FBW} = 91.4 \tag{13}$$

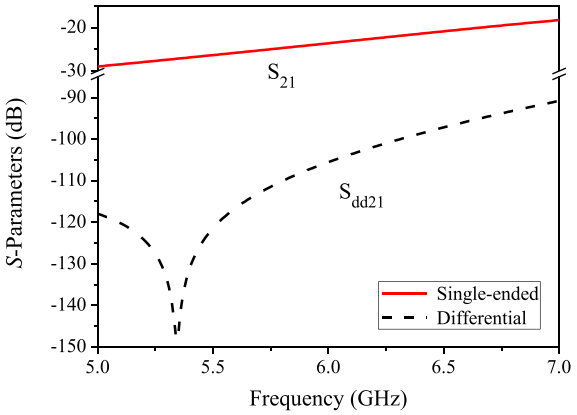

FIGURE 15. The simulated S-L coupling strengths of the BPFs in single-ended or differential types, as shown in Fig. 7 and Fig. 14, respectively.

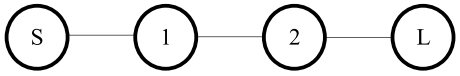

FIGURE 16. The coupling route of the proposed differential BPF.

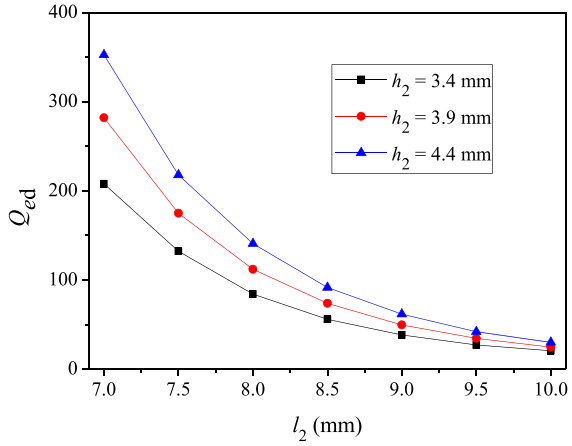

FIGURE 17. The relationship between Q_{ed} and l_2 under different h_2.

The extraction of k_{12d} is the same as that of k_{12} in the single-ended filter, as in Fig. 8. Meanwhile the extracted Q_{ed} is shown in Fig. 17.

B. RESULT AND DISCUSSION

According to the above description, the dimensions of the proposed DM BPF can be determined as: $A = 25$ mm, $H = 10$ mm, $a = 15$ mm, $b = 2.5$ mm, $t = 1$ mm, $h = 0.76$ mm, $h_2 = 3.9$ mm and $l_2 = 8.5$ mm. The simulation is conducted by using Ansoft HFSS, and the experiment is conducted by using Agilent N5230A PNA-L network analyzer, which can test four port S-parameters directly. Fig. 18 shows the simulated and measured S-parameters, showing good agreement. The measured DM passband is centered at about 5.8 GHz, and the 3-dB FBW is 1.62%. In the DM passband, the minimum insertion loss (S_{dd21}) is about 0.88 dB while the return loss

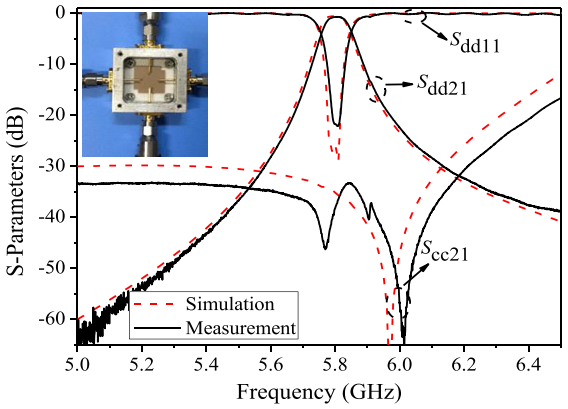

FIGURE 18. The simulated and measured frequency responses of the proposed differential BPF (The inset is the photograph of fabricated differential BPF).

(S_{dd11}) is better than 20 dB. The CM suppression (S_{cc21}) is more than 30 dB in the DM passband, which is acceptable in many applications.

TABLE 1. Units for magnetic properties.

Ref	f_0 (GHz)	3-dB FBW (%)	Insertion loss (dB)	CM Suppression (dB)	Volume (mm^3)
[19]	1.78	1.3	0.8	>30	45×45 ×53
[23]	1.75	1.3	0.4	>40	95×46 ×32
[25]	3.97	0.5	1.3	>25	62×40.8 ×12.3
This work	5.8	1.62	0.88	>30	25×25 ×10

Comparison of the proposed differential BPF using the DPR with reported second-order differential DR BPFs

Table 1 shows the comparison of the proposed differential BPF using the DPR with the previously-reported second-order differential DR BPFs. In [19] and [23], the Al_2O_3 support for the DR is required so that the filter profile is high. Since the cross-shaped dual-mode DR is applied in [19], the filter size is reduced dramatically, as compared with the DR filter in [23]. In [25], the TE_{11} mode of the rectangular DR mounted on the substrate is used. Though the profile is low, the longitudinal size is relatively large due to the single-mode operation of the DR. Benefiting from the proposed dual-mode DPR, the resultant differential BPF in this work owns evident volume reduction and the comparable filtering performance with the filters in [19], [23], and [25].

V. CONCLUSION

In this paper, a new square DPR has been introduced and theoretically analyzed. It has both merits of the planar transmission line and the traditional DR at the same time, i.e. low-profile configuration and high Q_u. For demonstration, two kind of filter examples based on the proposed DPR has been designed and presented in detail. Their simulated

and measured results with good agreement have been given, which effectively verify the proposed idea, both single-ended and differential BPFs showcase several advantages such as low passband loss, low profile and compact size, which would make the proposed DPR technique attractive in the future practical applications with the requirement of miniaturization.

REFERENCES

[1] K. W. Leung, E. H. Lim, and X. S. Fang, "Dielectric resonator antennas: From the basic to the aesthetic," *Proc. IEEE*, vol. 100, no. 7, pp. 2181–2193, Jul. 2012, doi: 10.1109/JPROC.2012.2187872.

[2] S. J. Fiedziuszko and S. Holme, "Dielectric resonators raise your high-Q," *IEEE Microw. Mag.*, vol. 2, no. 3, pp. 50–60, Sep. 2001, doi: 10.1109/6668.951549.

[3] C. Wang and K. A. Zaki, "Dielectric resonators and filters," *IEEE Microw. Mag.*, vol. 8, no. 5, pp. 115–127, Oct. 2007, doi: 10.1109/MMM.2007.903648.

[4] D. Kajfez and P. Guillon, *Dielectric Resonators*. Norwood, MA, USA: Artech House, 1986.

[5] J.-X. Chen, Y. Zhan, W. Qin, and Z.-H. Bao, "Design of high-performance filtering balun based on $TE_{01\sigma}$-mode dielectric resonator," *IEEE Trans. Ind. Electron.*, vol. 64, no. 1, pp. 451–458, Jan. 2017, doi: 10.1109/TIE.2016.2608788.

[6] V. Singh, K. S. Parikh, S. Singh, and R. B. Bavaria, "DR OMUX for satellite communications: A complete step-by-step design procedure for the C-band dielectric resonator output multiplexer," *IEEE Microw. Mag.*, vol. 14, no. 6, pp. 104–118, Sep./Oct. 2013, doi: 10.1109/MMM.2013.2269871.

[7] M. A. Ismail, D. Smith, A. Panariello, Y. Wang, and M. Yu, "EM-based design of large-scale dielectric-resonator filters and multiplexers by space mapping," *IEEE Trans. Microw. Theory Techn.*, vol. 52, no. 1, pp. 386–392, Jan. 2004, doi: 10.1109/TMTT.2003.820900.

[8] L. Zhou, W. Y. Yin, J. Wang, and L. S. Wu, "Dielectric resonators with high Q-factor for tunable low phase noise oscillators," *IEEE Trans. Compon. Packag. Manuf. Technol.*, vol. 3, no. 6, pp. 1008–1015, Jun. 2013, doi: 10.1109/TCPMT.2013.2258465.

[9] S. J. Ha, Y. D. Lee, Y. H. Kim, J. J. Choi, and U. S. Hong, "Dielectric resonator oscillator with balanced low noise amplifier," *Electron. Lett.*, vol. 38, no. 24, pp. 1542–1544, Nov. 2002, doi: 10.1049/el:20020993.

[10] L. K. Hady, D. Kajfez, and A. A. Kishk, "Dielectric resonator antenna in a polarization filtering cavity for dual function applications," *IEEE Trans. Microw. Theory Techn.*, vol. 56, no. 12, pp. 3079–3085, Dec. 2008, doi: 10.1109/TMTT.2008.2006806.

[11] S. Maity and B. Gupta, "Experimental investigations on wideband triangular dielectric resonator antenna," *IEEE Trans. Antennas Propag.*, vol. 64, no. 12, pp. 5483–5486, Dec. 2016, doi: 10.1109/TAP.2016.2607765.

[12] L. K. Hady, D. Kajfez, and A. A. Kishk, "Triple mode use of a single dielectric resonator," *IEEE Trans. Antennas Propag.*, vol. 57, no. 5, pp. 1328–1335, May 2009, doi: 10.1109/TAP.2009.2016708.

[13] S. Fakhte and H. Oraizi, "Compact uniaxial anisotropic dielectric resonator antenna operating at higher order radiating mode," *Electron. Lett.*, vol. 52, no. 19, pp. 1579–1580, Aug. 2016, doi: 10.1049/el.2016.2222.

[14] H. Tang, J.-X. Chen, W.-W. Yang, L.-H. Zhou, and W. Li, "Differential dual-band dual-polarized dielectric resonator antenna," *IEEE Trans. Antennas Propag.*, vol. 65, no. 2, pp. 855–860, Feb. 2017, doi: 10.1109/TAP.2016.2630661.

[15] L.-S. Wu, L. Zhou, X.-L. Zhou, and W.-Y. Yin, "Bandpass filter using substrate integrated waveguide cavity loaded with dielectric rod," *IEEE Microw. Wireless Compon. Lett.*, vol. 19, no. 8, pp. 491–493, Aug. 2009, doi: 10.1109/LMWC.2009.2024824.

[16] D.-D. Zhang, L. Zhou, L.-S. Wu, L.-F. Qiu, W.-Y. Yin, and J.-F. Mao, "Novel bandpass filters by using cavity-loaded dielectric resonators in a substrate integrated waveguide," *IEEE Trans. Microw. Theory Techn.*, vol. 62, no. 5, pp. 1173–1182, May 2014, doi: 10.1109/TMTT.2014.2314677.

[17] H. Hu and K.-L. Wu, "A TM_{11} dual-mode dielectric resonator filter with planar coupling configuration," *IEEE Trans. Microw. Theory Techn.*, vol. 61, no. 1, pp. 131–138, Jan. 2013, doi: 10.1109/TMTT.2012.2226741.

[18] I. C. Hunter, J. D. Rhodes, and V. Dassonville, "Dual-mode filters with conductor-loaded dielectric resonators," *IEEE Trans. Microw. Theory Techn.*, vol. 47, no. 12, pp. 2304–2311, Dec. 1999, doi: 10.1109/22.808975.

[19] J.-X. Chen, J. Li, W. Qin, J. Shi, and Z.-H. Bao, "Design of balanced and balun filters using dual-mode cross-shaped dielectric resonators," *IEEE Trans. Microw. Theory Techn.*, vol. 65, no. 4, pp. 1226–1234, Apr. 2017, doi: 10.1109/TMTT.2016.2635653.

[20] M. Memarian and R. R. Mansour, "Quad-mode and dual-mode dielectric resonator filters," *IEEE Trans. Microw. Theory Techn.*, vol. 57, no. 12, pp. 3418–3426, Dec. 2009, doi: 10.1109/TMTT.2009.2034310.

[21] A. Panariello, M. Yu, and C. Ernst, "Ku-band high power dielectric resonator filters," *IEEE Trans. Microw. Theory Techn.*, vol. 61, no. 1, pp. 382–392, Jan. 2013, doi: 10.1109/TMTT.2012.2229292.

[22] Q.-X. Chu, X. Ouyang, H. Wang, and F.-C. Chen, "$TE_{01\delta}$-mode dielectric-resonator filters with controllable transmission zeros," *IEEE Trans. Microw. Theory Techn.*, vol. 61, no. 3, pp. 1086–1094, Mar. 2013, doi: 10.1109/TMTT.2013.2238551.

[23] Y. Zhan, J. Li, W. Qin, and J.-X. Chen, "Low-loss differential bandpass filter using $TE_{01\sigma}$-mode dielectric resonators," *Electron. Lett.*, vol. 51, no. 13, pp. 1001–1003, Jun. 2015, doi: 10.1049/el.2015.0719.

[24] T. D. Iveland, "Dielectric resonator filters for application in microwave integrated circuits," *IEEE Trans. Microw. Theory Techn.*, vol. 19, no. 7, pp. 643–652, Jul. 1971, doi: 10.1109/TMTT.1971.1127594.

[25] J.-X. Chen, Y. Zhan, W. Qin, Z.-H. Bao, and Q. Xue, "Novel narrow-band balanced bandpass filter using rectangular dielectric resonator," *IEEE Microw. Wireless Compon. Lett.*, vol. 25, no. 5, pp. 289–291, May 2015, doi: 10.1109/LMWC.2015.2409805.

[26] H. W. Lai, K.-M. Luk, and K. W. Leung, "Dense dielectric patch antenna—A new kind of low-profile antenna element for wireless communications," *IEEE Trans. Antennas Propag.*, vol. 61, no. 8, pp. 4239–4245, Aug. 2013, doi: 10.1109/TAP.2013.2260122.

[27] Y. Li and K.-M. Luk, "A 60-GHz dense dielectric patch antenna array," *IEEE Trans. Antennas Propag.*, vol. 62, no. 2, pp. 960–963, Feb. 2014, doi: 10.1109/TAP.2013.2291558.

[28] O. M. Haraz, A. Elboushi, S. A. Alshebeili, and A.-R. Sebak, "Dense dielectric patch array antenna with improved radiation characteristics using EBG ground structure and dielectric superstrate for future 5G cellular networks," *IEEE Access*, vol. 2, pp. 909–913, 2014, doi: 10.1109/ACCESS.2014.2352679.

[29] J. S. Hong and M. J. Lancaster, *Microwave Filter for RF/Microwave Application*. Hoboken, NJ, USA: Wiley, 2001.

[30] R. J. Cameron, C. M. Kudsia, and R. R. Mansour, *Microwave Filters for Communication Systems*. Hoboken, NJ, USA: Wiley, 2007.

JIAN-XIN CHEN (M'08–SM'17) was born in Nantong, China, in 1979. He received the B.S. degree from the Huaiyin Teachers College, Jiangsu, China, in 2001, the M.S. degree from the University of Electronic Science and Technology of China, Chengdu, China, in 2004, and the Ph.D. degree from the City University of Hong Kong, Hong Kong, in 2008.

Since 2009, he has been with Nantong University, Nantong, China, where he is currently a Professor. He has authored or co-authored over 100 internationally referred journal and conference papers. He holds 15 Chinese patents and three U.S. patents. His research interests include RF/microwave differential circuits and antennas, dielectric resonator filters, and low temperature co-fired ceramic millimeter-wave circuits and antennas.

Dr. Chen was a recipient of the Best Paper Award presented at the Chinese National Microwave and Millimeter-Wave Symposium, Ningbo, China, in 2007. He was the Supervisor of 2014 iWEM student innovation competition winner, Sapporo, Japan. He was a TPC Co-Chair of IEEE iWEM in 2016. He has been a regular reviewer for several international journals, including four IEEE TRANSACTIONS.

YUN-LI LI was born in Jiangsu, China, in 1992. He received the B.Sc. degree from Southeast University, Nanjing, China, in 2014. He is currently pursuing the M.Sc. degree in electromagnetic field and microwave technology from Nantong University, Nantong, China.

His current research interests include microwave filters and diplexer.

WEN-WEN YANG received the B.Eng. degree in information engineering, the M.Eng. and Ph.D. degrees in electrical engineering from Southeast University, Nanjing, China, in 2007, 2010, and 2015, respectively. He is currently with the School of Electronics and Information, Nantong University, Nantong, China, as a Lecturer.

His research interests include RF, microwave and millimeter-wave passive devices, active antenna array, and antennas for wireless communication. He serves as a Reviewer for several journals, including the IEEE TRANSACTIONS ON ANTENNAS AND PROPAGATION, IET MAP, and EL.

ZHI-HUA BAO was born in Nantong, Jiangsu, China, in 1955. He received the B.S. degree from Chongqing University, Chongqing, China, in 1982, and the M.S. degree from the Nanjing University of Posts and Telecommunications, Nanjing, China, in 1985.

In 1988, he joined Nantong University as a Lecturer, where he is currently a Professor with the School of Electronics and Information. He has authored or co-authored over 60 journal papers. He has owned four Chinese patents. His research interests include modern communication theory and technology, communications-specific integrated circuit designs, and RF/microwave active and passive circuits.